DOE GRANT NO. : DE-FG26-99FT40595

SO_2 REMOVAL WITH COAL SCRUBBING

Final Report

Aug 1, 1999
through
July 31, 2001

Prepared by

Eung Ha Cho
Hari Prashanth Sundaram
Aubrey L. Miller

July 2001

Submitted by:

Department of Chemical Engineering
West Virginia University
P.O. Box 6102
Morgantown, WV 26506

DISCLAIMER

This report was prepared as an account of work sponsored by an agency of the United States Government. Neither the United States Government nor any agency thereof, nor any of their employees, makes any warranty, expressed or implied, or assumes any legal liability or responsibility for the accuracy, completeness, or usefulness of any information, apparatus, product, or process disclosed, or represents that its use would not infringe privately owned rights. Reference herein to any specific commercial product, process, process, or service by trade name, trademark, manufacturer, or otherwise does not necessarily constitute or imply its endorsement, recommendation, or favoring by the United States Government or any agency thereof. The views and opinions of authors expressed herein do not necessarily state or reflect those of the Unites States Government or agency thereof.

ABSTRACT

This project is based on an effective removal of sulfur dioxide from flue gas with coal as the scrubbing medium instead of lime, which is used in the conventional FGD processes. A laboratory study proves that coal scrubbing is an innovative technology that can be implemented into a commercial process in place of the conventional lime scrubbing flue gas desulfurization process. SO_2 was removed from a gas stream using an apparatus, which consisted of a 1- liter stirred reactor immersed in a thermostated oil bath. The reactor contained 60 g of 35-65 mesh coal in 600 ml of water. The apparatus also had 2 bubblers connected to the outlet of the reactor, each containing 1500 ml of 1 molar NaOH solution. The flow rate of the gas was 30 ml/sec, temperature was varied from 21^0C to 73^0C. Oxygen concentration ranged from 3 to 20% while SO_2 concentration, from 500 to 2000 ppm. SO_2 recovery was determined by analyzing SO_2 concentration in the liquid samples taken from the bubblers. The samples taken from the reactor were analyzed for iron concentrations, which were then used to calculate fractions of coal pyrite leached.

It was found that SO_2 removal was highly temperature sensitive, giving 13.1% recovery at 21^0C and 99.2% recovery at 73^0C after 4 hours. The removal of SO_2 was accomplished by the catalysis of iron that was produced by leaching of coal pyrite with combination of SO_2 and O_2. This leaching reaction was found to be controlled by chemical reaction with apparent activation energy of 11.6 kcal/mole. SO_2 removal increased with increasing O_2 concentration up to 10% and leveled off upon further increase. The effect of SO_2 concentration on its removal was minimal.

ACKNOWLEDGEMENTS

To the Faculty and Staff of the Department of Chemical Engineering for their help and support provided for this project.

The author also wishes to express his appreciation to the United States Department of Energy, National Energy Technology Laboratory for financial support received under Grant DE-FG26-99FT40595, which made this research project possible.

TABLE OF CONTENTS

LIST OF FIGURES

LIST OF TABLES

INTRODUCTION

This thesis deals with scrubbing of flue gas to remove SO_2 using coal as the scrubbing medium in place of lime, which is used in the lime-scrubbing desulfurization process. The idea is based on a chemistry in which the combination of SO_2 and O_2 has an oxidizing power to leach coal pyrite, and one of the oxidation products, ferric ion, can subsequently catalyze the oxidation of incoming SO_2. This process can serve two purposes: one is to capture SO_2 and oxidize it to sulfate ion, which is an advantage over the conventional lime scrubbing, and the other is to reduce pyritic sulfur from coal.

Although many innovative stack gas desulfurization processes have been developed especially in recent years, lime scrubbing may still be considered as the standard stack gas desulfurization process. The reason is that lime scrubbing still makes most of the stack gas desulfurization plants in the world. One of the shortcomings of this process is that it produces calcium sulfate ($CaSO_3$), which renders huge problems connected with sludge handling and waste disposal. Another problem may be that the reaction rate between SO_2 and lime/limestone is slow, thus requiring a long retention time and tall reactor, which results in an expensive operation particularly in terms of pumping the slurry. The average SO_2 recovery among various types of reactors is about 78%, which is due to the slow reaction rate between SO_2 and lime/limestone.[1] Moreover, small particle size of lime/limestone is needed to increase the total surface area and thus the SO_2 recovery.[1] Again, more lime/limestone is used in comparison with its stoichiometric amount in order to increase the SO_2 recovery. This value runs between 100 to 300%.[1] These two factors undoubtedly render a disadvantage to the lime/limestone scrubbing processes.

On the other hand, scrubbing of flue gas to remove SO_2 using coal as the scrubbing medium in place of lime can eliminate this problem because SO_2 is oxidized to sulfate ion and marketable calcium sulfate is produced upon manipulation of the process.

The catalysis of ferric/ferrous ions for the reaction between SO_2 and O_2 has been known for many years. One of the applications is the Chiyoda process (CT-101)[2] which oxidizes the incoming SO_2 using mine water which contains ferric/ferrous ions. The oxidation reactions occur by three routes.[3] First, SO_2 serves as a reducing reagent of ferric ion as

$$SO_2 + 2Fe^{3+} + 2H_2O \rightarrow SO_4^{2-} + 4H^+ + 2Fe^{2+} \quad (1)$$

Second, SO_2 together with O_2 serves as an oxidizing reagent of ferrous ion to ferric ion as

$$SO_2 + O_2 + 2Fe^{2+} \rightarrow SO_4^{2-} + 2Fe^{3+} \quad (2)$$

Third, ferric ion catalyzes the oxidation reaction of SO_2 as

$$SO_2 + H_2O + \tfrac{1}{2}O_2 \rightarrow SO_4^{2-} + 2H^+ \quad (3)$$

The Chiyoda process was abandoned because the supply of mine water to the plant site seemed to be the problem. However ferric/ferrous ions can be produced in situ by a chemical reaction, that is by leaching of coal pyrite with a combination of SO_2 and O_2. This is possible because the combination of SO_2 and O_2 is a strong oxidation reagent. The leaching of sulfide minerals with the combination of SO_2 and O_2 are well documented in the literature.[4,5]

It is reported that mineral pyrite exhibits a high rest potential of 0.62 eV (rest potential is corrosion potential with a given oxidizing reagent), which is more noble than any other sulfide mineral.[6] However, it has been reported that mineral pyrite is vastly different from coal pyrite in reactivity due to their surface structure and morphology.[7]

The study revealed that oxidation rate of coal pyrite was twice as high as that of mineral pyrite at 5% oxygen; and four times as high as that of mineral pyrite at 10% oxygen. Thus, it can be surmised that coal pyrite can be leached at a faster rate than mineral pyrite.

The dissolution of coal pyrite in the presence of SO_2 and O_2 can be analyzed thermodynamically as follows: The dissolution reaction is based on an electrochemical reaction. The anodic reaction is

$$FeS_2 + 8H_2O \rightarrow Fe^{2+} + 2SO_4^{2-} + 16H^+ + 14e^- \quad E^0(\text{for cathodic reaction}) = 0.355 \text{ eV} \quad (4)$$

The cathodic reaction may be written as

$$H_2SO_3 + O_2 + 2e \rightarrow SO_4^{2-} + H_2O \qquad E^0 = 2.29 \text{ eV} \qquad (5)$$

where H_2SO_3 represents the aqueous SO_2 which is predominant at low pHs. It can be seen from Equation (4) and Equation (5) that the difference in E^0 between cathodic and anodic reactions is huge, suggesting that the leaching reaction is thermodynamically very spontaneous under normal conditions. The overall reaction can be written as

$$FeS_2 + H_2O + 7\,H_2SO_3 + 7O_2 \rightarrow Fe^{2+} + 9SO_4^{2-} + 16H^+ \qquad \Delta G^0 = -624.7 \text{ kcal/mol} \quad (6)$$

Again the magnitude of the standard free energy suggests that the leaching reaction is thermodynamically spontaneous under normal conditions.

The objective of the present study is to determine the effects of temperature, oxygen concentration, and SO_2 concentration on SO_2 removal from simulated flue gas streams and on leaching rate of coal pyrite.

EXECUTIVE SUMMARY

Currently lime scrubbing flue gas desulfurization (FGD) process is considered to be the standard FGD process because it makes the most of the FGD processes in the world. However, the process has some shortcomings because of "low" reaction rate between lime particle and SO_2 gas. This results in building a tall reactor (e.g., 100 feet) to increase the reaction time and thus the removal percent. This also results in using an amount of lime 1.5 times as much as its stoichiometric amount. Another shortcoming of the lime scrubbing FGD process is that it produces calcium sulfite ($CaSO_3$) which renders huge problems connected with sludge handling and waste disposal.

This project was conducted to remove SO_2 from flue gas using coal as the scrubbing medium. SO_2 was removed in laboratory experiments from a gas stream using an apparatus which included a 1- liter stirred reactor containing 60 g of 35-65 mesh coal in 600 ml of water. The flow rate of the gas was 30 ml/sec, temperature was varied from 21^0C to 73^0C. Oxygen concentration ranged from 3 to 20% while SO_2 concentration, from 500 to 2000 ppm. It was found that SO_2 removal was highly temperature sensitive, giving 13.1% recovery at 21^0C and 99.2% recovery at 73^0C after 4 hours. The removal of SO_2 was accomplished by the catalysis of iron that was produced by leaching of coal pyrite with combination of SO_2 and O_2. This leaching reaction was found to be controlled by chemical reaction with apparent activation energy of 11.6 kcal/mole.

It can be concluded that our process, FGD with coal scrubbing, is an innovative technology that can be implemented into a commercial process in place of the conventional lime scrubbing flue gas desulfurization process. As has been found from a laboratory investigation, the oxidation rate of SO_2 is so fast to give more than 98%

removal of the gas, and thus there would be no problems connected with low reaction rate as mentioned previously in the lime scrubbing FGD process. The calcium sulfite problems would no longer be the case with our process because our process produces sulfate ion directly that can easily be converted to marketable gypsum or calcium sulfate.

This new technology can be implemented into a feasible commercial process. It is to retrofit into an existing lime scrubbing process. This retrofitting seems to offer the best of economical advantage because there is no need to build a new reactor.

EXPERIMENTAL

A raw coal sample of Pittsburgh No. 8 coal was obtained from Anker Energy. The sample was crushed and screened to produce a minus 28 mesh fraction. This fraction was cleaned by the conventional flotation technique. The concentrate was dried and screened again to produce 35-65 mesh fraction, which was used for the experiments in the study. The chemical analysis of this coal fraction showed that it contained 0.13% non-pyritic iron and 1.08% pyritic iron. The ash in the coal was determined to be 7.5%.

The apparatus consisted of three gas tanks (nitrogen, oxygen and 1% SO_2), a one liter reactor, and two bubblers which were connected in series as shown in Figure 1. The reactor was immersed in a thermostated, constant-temperature bath. It had four necks: the central neck was equipped with a stirrer connected to a motor operating at a speed of 470-500 rpm. One of the three side necks was fitted with a condenser, the next with a bubbler, and the last with a sample-taking device. The gases, after being metered for their flow rates, were combined in a gas mixer. The gases were then introduced into the reactor and bubbled through the coal slurry added to the reactor. SO_2 was dissolved and reacted with coal pyrite, the undissolved SO_2 exited the reactor and was captured in the bubblers. Each bubbler contained 1.5 liters of 1 molar NaOH solution. The pressure inside the reactor was increased above the atmospheric pressure because of the backpressure added by the two bubblers. The average pressure inside the reactor was measured to be 1.26 atmospheres.

Two types of experiments were conducted. One was for dissolution of SO_2 and the other was for removal of SO_2 with coal. Experiments for dissolution of SO_2

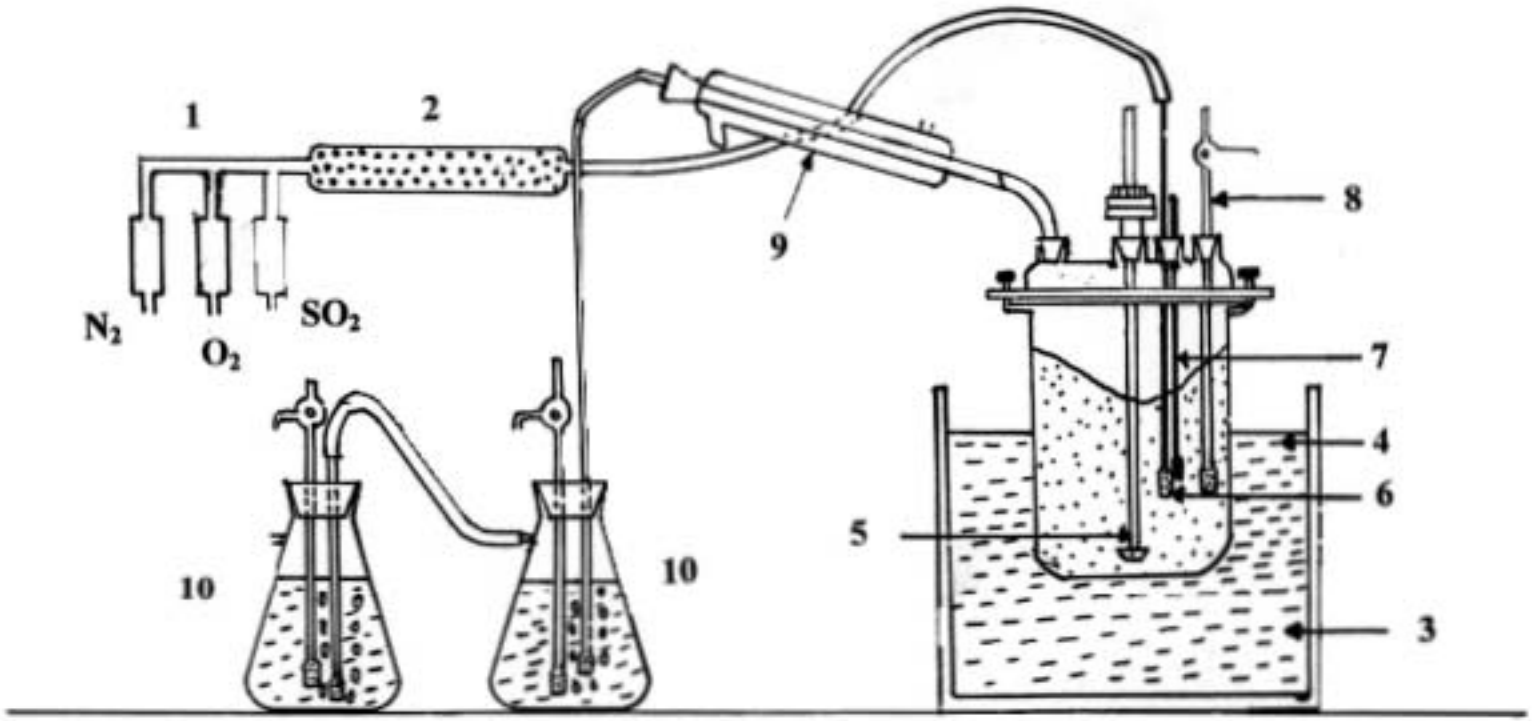

1. Flow meters
2. Gas mixer
3. Constant temp. oil bath
4. Reactor
5. Stirrer
6. Gas bubbler
7. Thermometer
8. Sample taking device
9. Condenser
10. Bubbler

Figure 1. Experimental apparatus

were carried out at various rpm (390, 472, 504) and at various temperatures (21, 57 and 71ºC). The flow rate of gas was 30 ml/sec. The gas stream had 2000 ppm SO_2 and 10% oxygen with the balance being nitrogen. The reactor contained 600 ml of de-ionized water. Approximately 15 ml samples were taken from the reactor every 12 to 15 minutes and analyzed for SO_2 concentration. The experiments lasted for 60 to 90 minutes. At the end of the experiment, approximately 15 ml sample was taken from each bubbler and analyzed for SO_2 to determine the mass balance on SO_2.

Experiments for removal of SO_2 were conducted with 60 grams of coal added to the 600 ml in the reactor. These experiments were carried out in order to determine the effects of various parametric conditions on the removal of SO_2 and leaching rate of coal pyrite. The temperatures were 21, 41, 59 and 73ºC. The flow rate of the gas stream and the stirring speed were the same as before. SO_2 concentration was varied from 500 to 2000 ppm while O_2 concentration, from 3 to 20%. Each experiment lasted for 4 hours. Two samples, one from each bubbler having approximately 15 ml were taken every one hour and analyzed for SO_2. Similarly, approximately 15 ml samples were taken from the reactor every hour and filtered before they were properly diluted and analyzed for iron concentration with a Perkin-Elmer model 2380 atomic absorption unit.

SO_2 was analyzed by a back titration method.[8] An excessive amount of iodine solution was added to each sample, and acidified if necessary. Then the SO_2 reacted with iodine and the unreacted iodine was titrated with sodium thiosulfate solution using an indicator of starch. Pyritic iron and non-pyritic iron in the coal were analyzed using the ASTM D 2492-84 method[9] while coal ash was analyzed using the ASTM D 3174-82 method.[10]

RESULTS

Table 1 gives removal data of SO_2 at various temperatures. The experimental conditions were 2000 ppm SO_2 and 10% oxygen. The removal values given in Table 1 are for each hour interval. It can be seen that at higher temperatures of 59 and 73ºC, the removal values are well above 90% throughout. At 41ºC, the removal for the first hour is higher than 90% but decreases drastically as time goes on. At 21ºC, the removal for the first hour is 64.1% but the values decrease even more drastically thereafter and reach negative values for the last two intervals. The high removal values at 21 and 41ºC for the first hour may be mainly due to adsorption of SO_2 on coal surface.

Table 1. Removal of Incoming SO_2 at various Temperatures (O_2=10%,SO_2=2000ppm)

Removal (%)					
Temp. (°C)	pH	Time			
		0-1 hr	1-2 hr	2-3 hr	3-4 hr
21	2.2	64.1	3.3	-1.1	-14.1
41	1.9	97.9	47.3	18.3	7.8
59	1.5	98.7	97.4	94.3	94.4
73	1.3	100.0	100	97.9	98.8

The negative values of removal at 21ºC may be explained as follows: The leaching reaction produces hydrogen ion as can be seen from Eq. (6). Since the solubility of SO_2 decreases with increasing hydrogen ion concentration, the equilibrium SO_2 concentration should decrease with time. If the value which is produced by subtracting the combination of equilibrium SO_2 concentration and equivalent oxidized SO_2

concentration from the actual SO_2 concentration is positive, SO_2 will bubble out of the reactor and the SO_2 removal will be negative. This is the case at 21ºC in the later stage because the oxidation rate of SO_2 is low. At higher temperatures, the oxidation rate of SO_2 is higher, thus the value mentioned previously will be negative which makes the SO_2 removal positive.

There is another aspect of the reaction to be noted which is pH of the coal slurry at various temperatures. The pH of the slurry at 4 hours was recorded to be 2.2 at 21ºC, 1.9 at 41ºC, 1.5 at 59ºC, and 1.3 at 73ºC. These values are expected because the pyrite leaching reaction is an acid-producing reaction as can be seen from Eq. (6). The decreasing values of the pH as temperature increases are the results from the increased pyrite leaching conversions.

Figure 2 shows a plot of the overall removal of SO_2 at four different temperatures. The overall removal was the cumulative value for 4 hours of the interval removal values given in Table 1. As can be seen from Figure 2, the overall removal values were 13.1% at 21ºC, 42.8% at 41ºC, 96.2% at 59ºC, and 99.2% at 73ºC. This figure suggests that SO_2 oxidation is temperature sensitive and should be carried out above 59ºC in order to achieve more than 90% SO_2 removal under the conditions applied.

Figure 3 shows a plot of iron concentration produced as a function of time. The experiments were the same as for Table 1 and Figure 2. One can see from Figure 3 that iron was produced favorably at high temperatures of 59 and 73ºC. These results are reflected on the data of SO_2 removal given in Table 1. Thus, one can conclude that SO_2 oxidation takes place as a result of iron production by leaching coal pyrite.

.

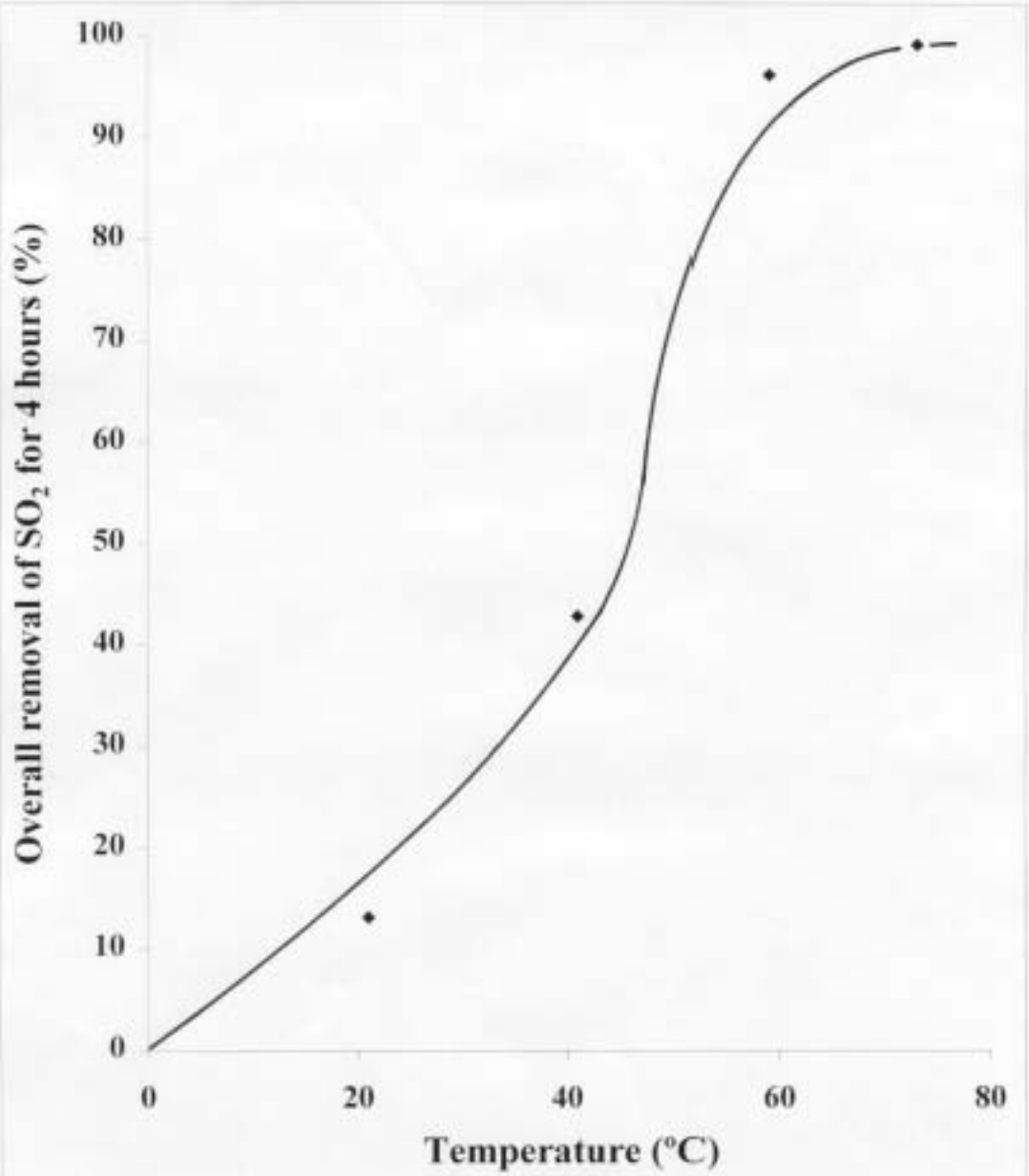

Figure 2. Overall removal of SO_2 for 4 hours at various temp. (O_2=10%,SO_2=2000ppm)

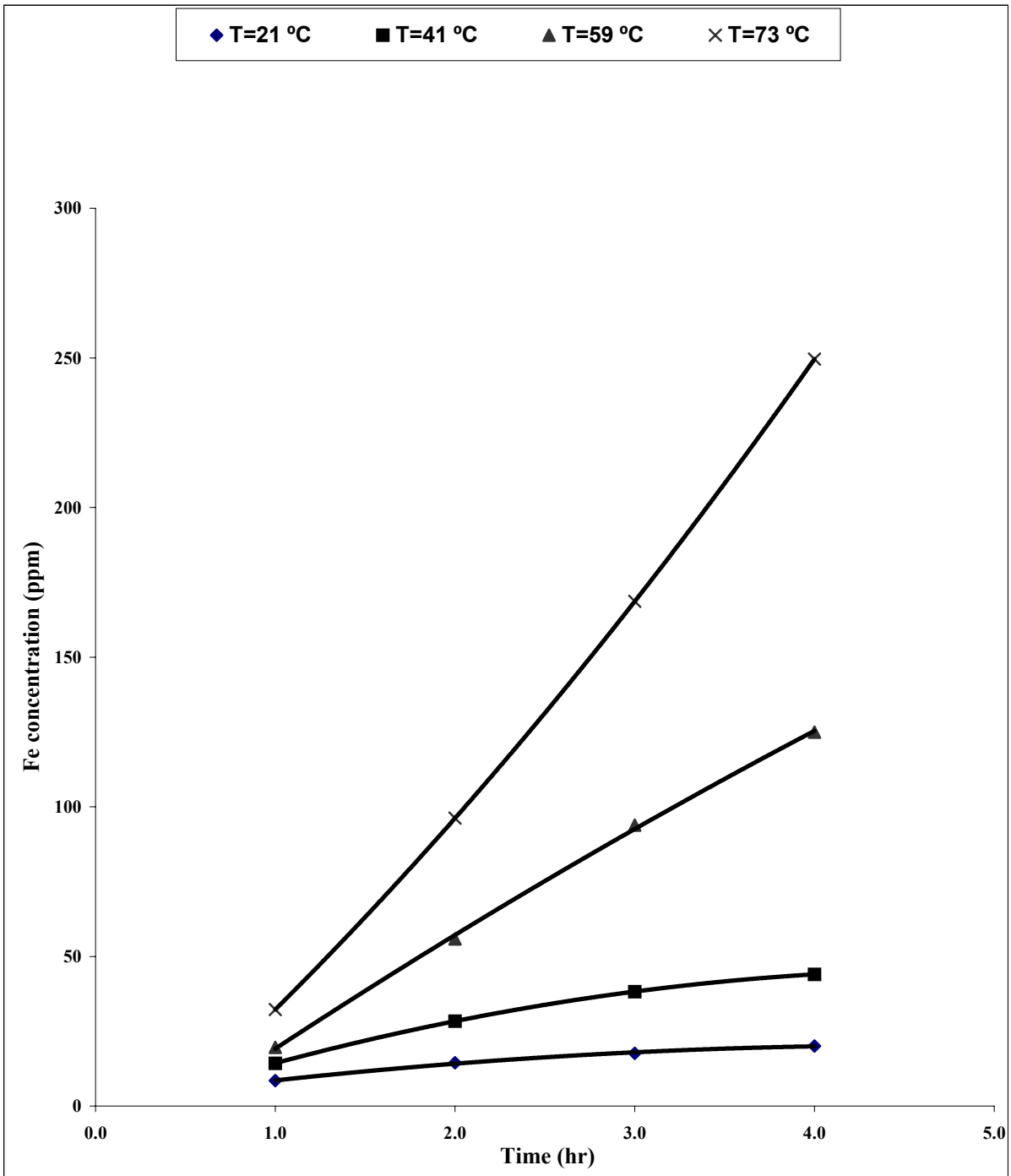

Figure 3. Plot of Fe conc. vs. time for various temperatures (SO_2=2000ppm,O_2=10%)

The data of Table 1 and Figure 3 reveal that only low concentrations of iron are needed to capture SO_2 very effectively in the early stages of reaction. For example, only 32.3 ppm of iron was needed to capture 100% SO_2 at 73ºC during the first hour, and only 19.6 ppm of iron was needed to capture 98.7% SO_2 at 59ºC during the first hour. Although the iron concentration increased to 253 ppm at 73ºC after 4 hours, the SO_2 removal decreased slightly. This may be because an increase in the concentration of sulfate ion in the solution due to the oxidation of SO_2 decreases the concentration of Fe^{3+} ion by forming complex ions such as $FeSO_4^+$, $Fe(SO_4)_2^-$ and $FeHSO_4^{2+}$.

Table 2 provides SO_2 removal data at various oxygen concentrations. Temperature was 73ºC and SO_2 was 2000 ppm. The removal values are those for 1-hour time intervals as in Table 1. Figure 4 is a plot for the overall SO_2 removal values for 4 hours at various oxygen concentrations. As one can see from Table 2 and Figure 4, the SO_2 removal increases with increasing O_2 concentration up to 10% and levels off upon further increase.

Table 2. Removal of Incoming SO_2 at Various O_2 Concentrations (Temp.= 73ºC, SO_2=2000ppm)

Removal (%)				
$[O_2]$ (%)	Time			
	0-1 hr	1-2 hr	2-3 hr	3-4 hr
3	92.8	89.6	88.3	93.6
6	100.0	98.4	95.2	96.3
10	100.0	100.0	97.9	98.8
20	100.0	100.0	100.0	100.0

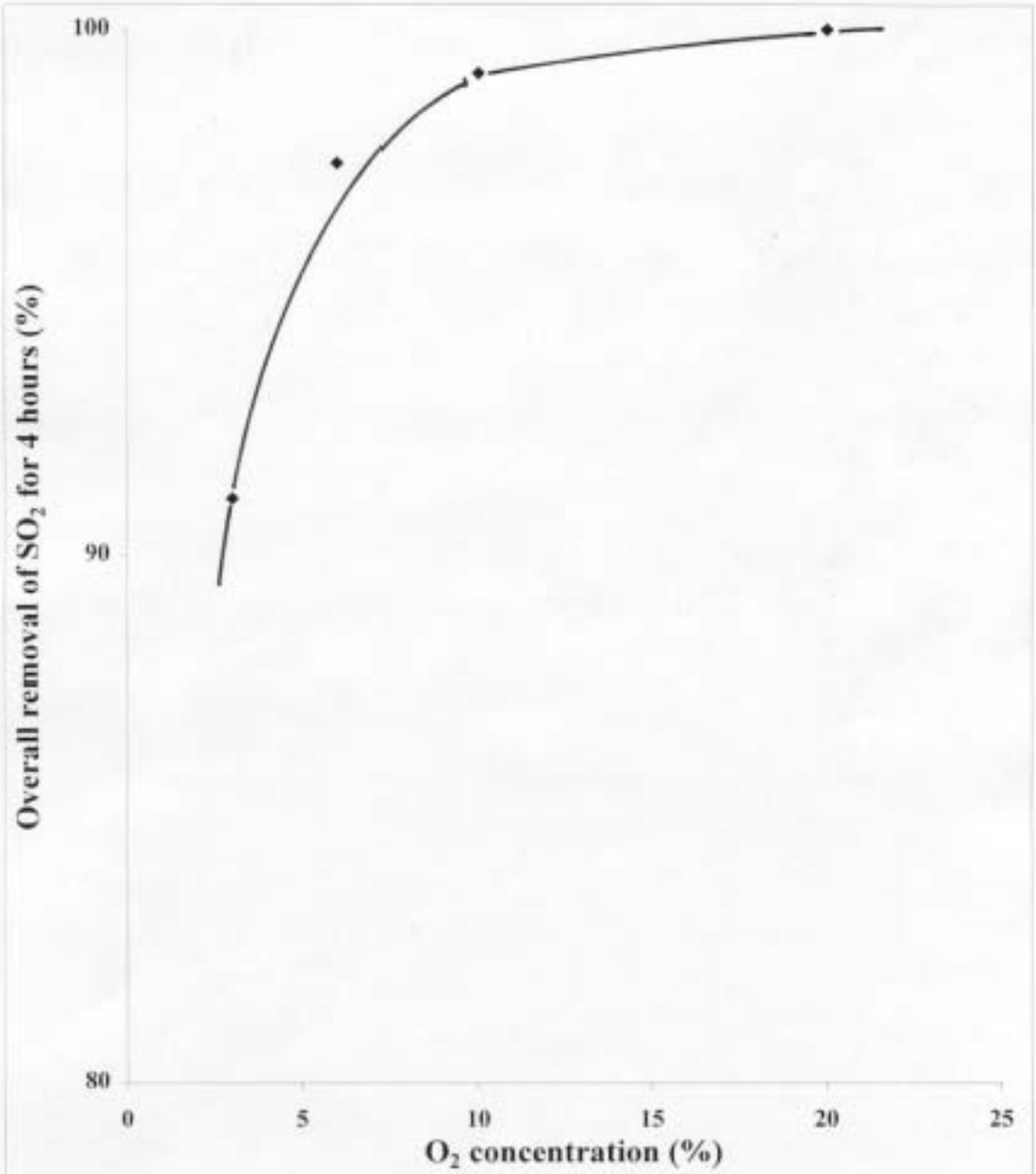

Figure 4. Overall removal of SO_2 for 4 hours at various O_2 conc. (Temp.=73°C,SO_2=2000ppm)

The effect of SO_2 concentration on its removal can be seen from Table 3 with interval removal values, and from Figure 5 with overall removal values. The experimental conditions were 73ºC and 10% oxygen. The data from the two sources reveal that there is a little or no effect of SO_2 concentration on its removal.

Table 3. Removal of Incoming SO_2 at Various SO_2 Concentrations (O_2=10%,Temp.= 73ºC)

Removal (%)				
$[SO_2]$ (ppm)	Time			
	0-1 hr	1-2 hr	2-3 hr	3-4 hr
500	100.0	100.0	99.1	99.2
1000	98.3	99.6	97.8	97.6
2000	100.0	100.0	97.9	98.8

From the above experiments it was found that a minimum of 20 ppm of iron was needed to achieve removals above 95% at high temperatures like 59 and 73ºC. However, at lower temperatures, high removals of SO_2 could not be achieved even with the iron concentration as high as 43 ppm.

The results for the experiments conducted to determine the dissolution rates of SO_2 are shown in Figure 6 and Table 4. The dissolution rate of SO_2 was first determined at various rpm. Figure 7 shows the results, from which we can see there is no rpm effect between 390 and 472 rpm, but the dissolution rate of SO_2 at 504 rpm is somewhat different from those at the other two rpm. These results reveal that the rpm effect is inconclusive. However, considering the general trend with the variation of rate constant

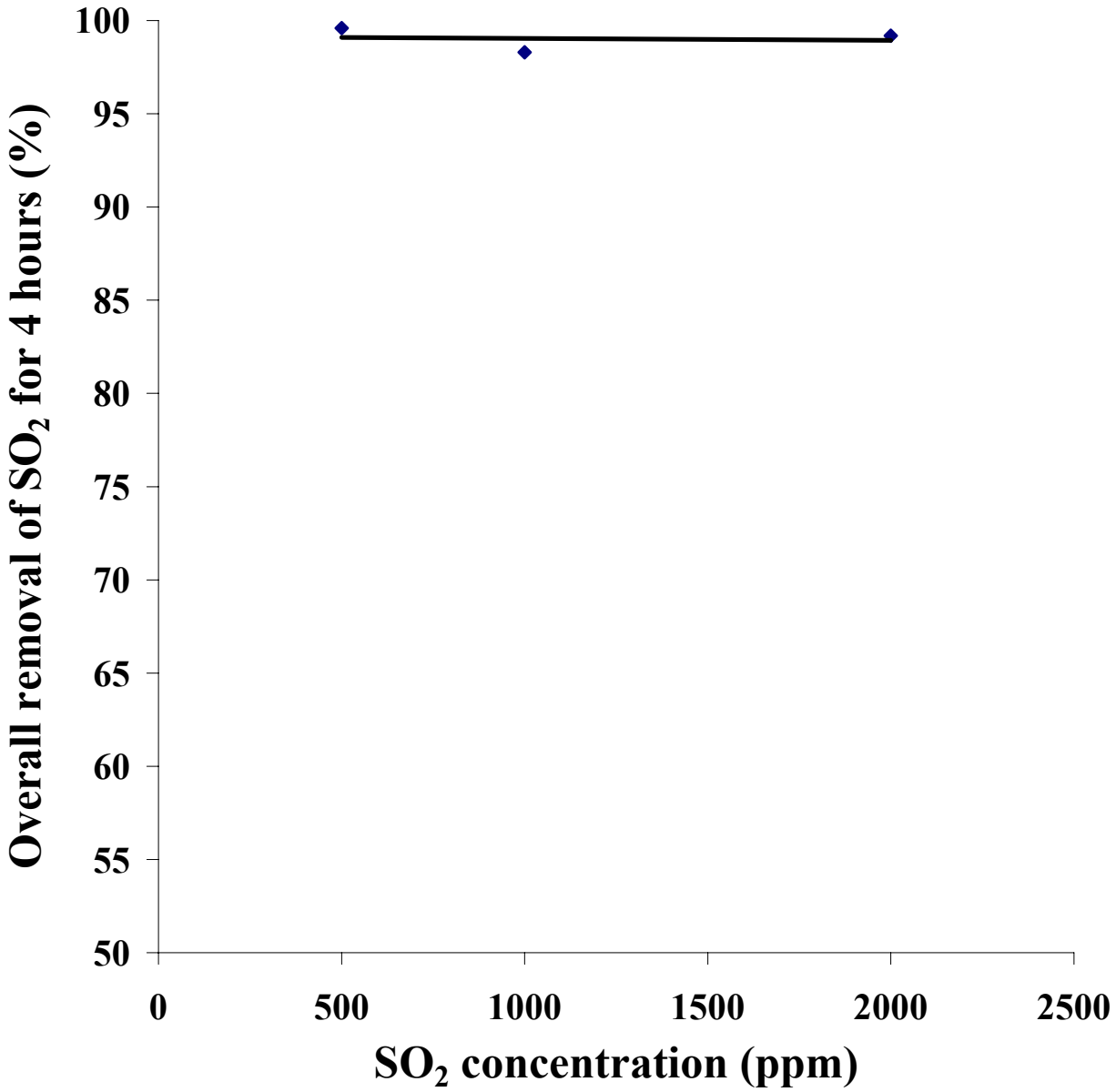

Figure 5. Overall removal of SO_2 for 4 hours at various SO_2 conc. (Temp.=73°C,O_2=10%)

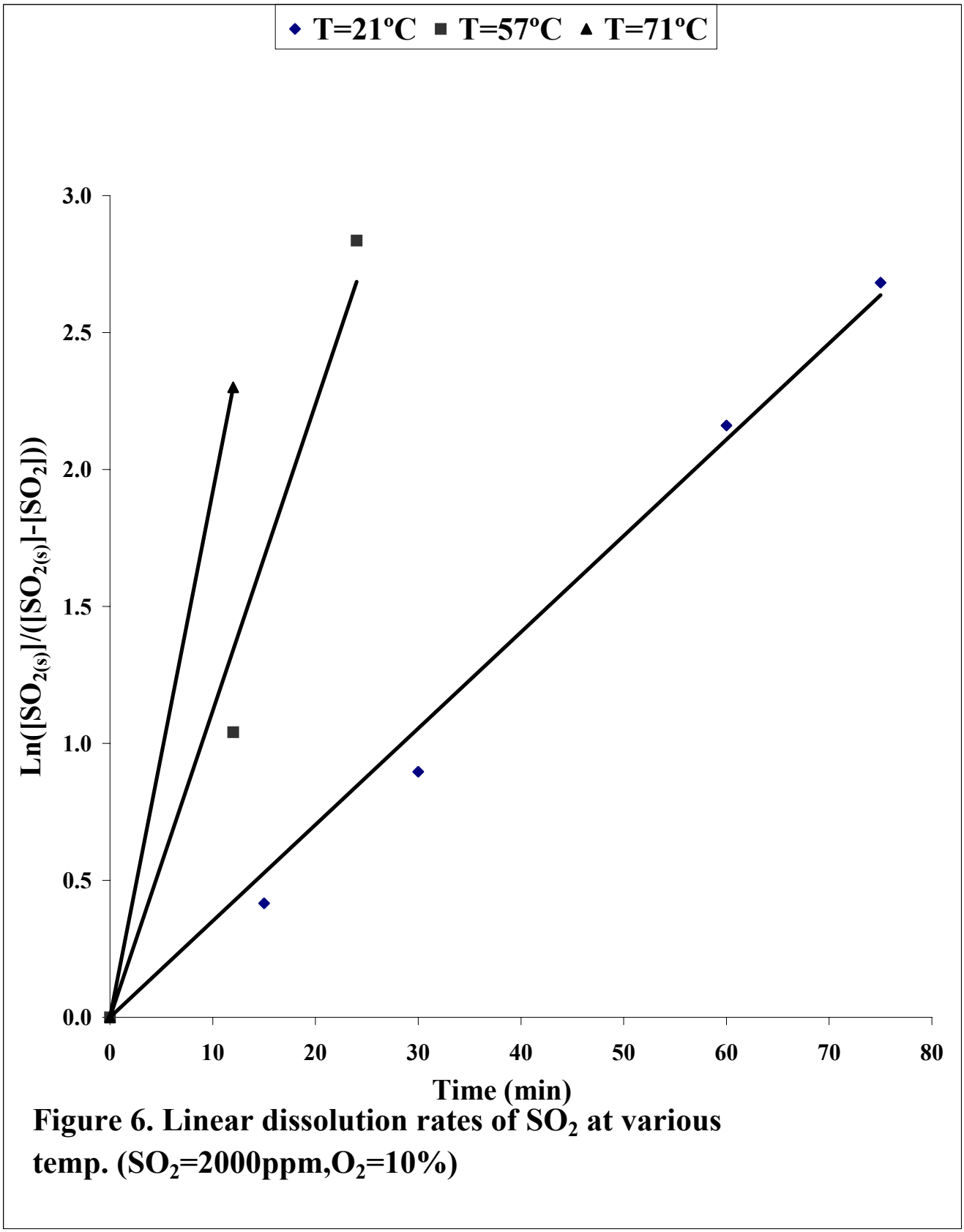

Figure 6. Linear dissolution rates of SO_2 at various temp. (SO_2=2000ppm,O_2=10%)

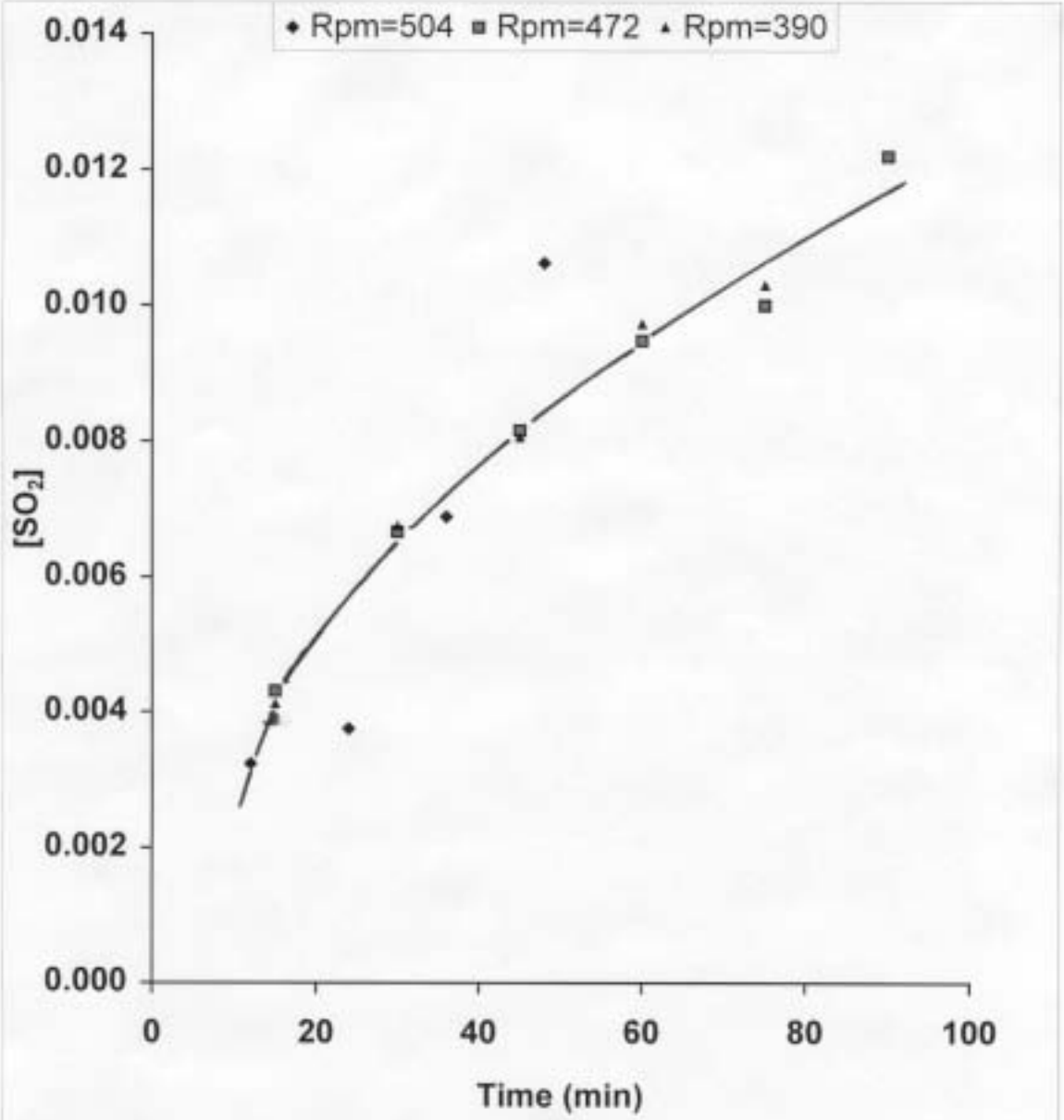

Figure 7. Conc. of dissolved SO_2 Vs time at various rpm (SO_2=2000ppm,O_2=10%,temp. =21°C)

as a function of rpm, we can surmise that the data at 504 rpm are due to some experimental errors and thus, we can say that there would not be any rpm effect in the specified rpm range.

Table 4. The values of $S \times k_l/V$ and $[SO_{2(s)}]$ at Various Temperatures

Temperature (ºC)	$S \times k_l/V$ (min^{-1})	$[SO_{2(s)}]$ (molar)
21	0.0334	0.0107
57	0.0809	0.0030
71	0.1916	0.0017

Presuming that the dissolution rate of SO_2 is controlled by the mass transfer of dissolved SO_2 in the liquid-boundary film in the rising gas bubbles, the following equation is obtained:

$$\frac{d[SO_2]}{dt} = \frac{S \times k_l}{V}\left([SO_{2(s)}] - [SO_2]\right) \tag{7}$$

where

$[SO_2]$ = concentration of dissolved SO_2, molar

$[SO_{2(s)}]$ = saturation concentration of dissolved SO_2, molar

V = solution volume, cm^3

S = total surface area of gas bubbles, cm^2

k_l = liquid-film mass transfer coefficient, cm/min

The experiments for the dissolution of SO_2 in a water medium were conducted at a constant stirring speed and at a constant gas flow rate. The pH was not maintained constant during the dissolution of SO_2. The pH values at the saturation of SO_2 were near

2.5. Assuming that the saturation concentration of SO_2 is the same at 2.5 and 5.5(natural pH), we should be able to integrate Eq. (7) into the form

$$\ln \frac{[SO_{2(s)}]}{[SO_{2(s)}]-[SO_2]} = \frac{S \times k_l}{V} t \qquad (8)$$

Experimental results for the dissolution of SO_2 are illustrated in Figure 6, plotted according to Eq. (8). The straight lines at the two lower temperatures are those of linear regression. At 71ºC, there is only one data point. This was because the dissolution rate was so fast that only two samples could be taken before SO_2 concentration reached its saturation. One can see from the figure that the data points are somewhat scattered from the straight lines. The way the data points are scattered seems to be due to the decrease in $[SO_{2(s)}]$ as time proceeds and at the same time the pH decreases.

The slope of the straight lines of Figure 6 gives a value of $S \times k_l/V$ which permits the rate constant of the dissolution to be calculated. Table 4 presents the values of this constant and the saturation concentrations of dissolved SO_2, which were obtained directly from the experiments at the various temperatures. The rate constant values are the average values in the pH range between 2.5 and 5.5. One can see from the values in Table 4 that the rate constant increases with increasing temperature and the saturation concentration of dissolved SO_2 decreases with increasing temperature.

The SO_2 dissolution experiments were conducted at 2000 ppm SO_2 and 10% oxygen. Mass balance on SO_2 for each experiment was made and it was validated with a minimum 90% accuracy.

DISCUSSION

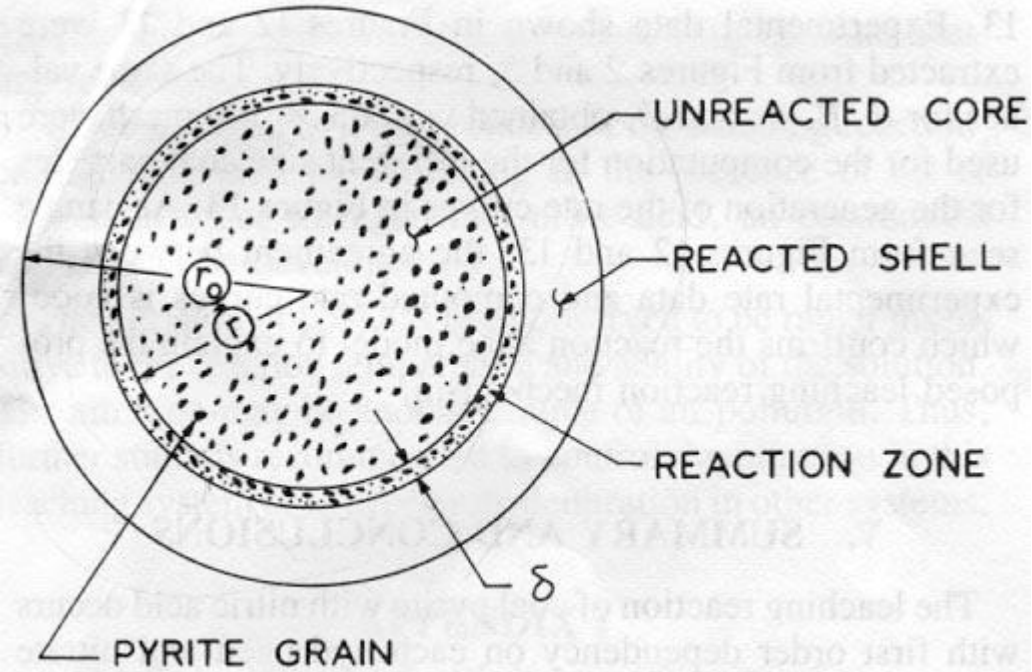

Fig. 8 – Coal particle of radius r_0, showing reaction zone.

Reaction Zone Model

The reaction zone model is based on a shrinking core model in which a reaction zone in the reaction interface moves inwards.[11] Figure 8 represents an idealized coal particle showing the reacted shell, unreacted core, and reaction zone. Pyrite grains are disseminated in the unreacted core of the coal particle and are subject to leaching in a reaction zone. The reaction zone may be viewed as a region in which disseminated pyrite grains are in all stages of reaction. As the zone moves to smaller values of r, unreacted pyrite grains are included in the zone. At the outer edge of the zone, the last vestige of unreacted pyrite disappears. Within the moving reaction zone, the concentration of chemical reagents and pyrite grains may be considered essentially constant. The reaction

zone model used in the present study is based on a control mechanism by chemical reactions. The leaching rate based on chemical reactions within the zone may be given as

$$\frac{dn}{dt} = -\frac{4\pi r^2}{\phi}\delta n_g A_g [SO_2]^p [O_2]^q k \tag{9}$$

where

n = number of moles of unleached pyrite in a coal particle at time t, (mol)

p = reaction order with respect to $[SO_2]$

q = reaction order with respect to $[O_2]$

δ = reaction zone thickness, (cm)

n_g = number of pyrite grains per unit volume of coal in the reaction zone, (cm^{-3})

A_g = average surface area of a pyrite grain, (cm^2)

k = rate constant

$[SO_2]$ and $[O_2]$ = concentrations of SO_2 and O_2 in the reaction zone, respectively, (mol/lit)

ϕ = sphericity of coal particle

The unit of k, rate constant, depends on the reaction orders of p and q. For example, if each p and q is half-order as will be shown later, the unit of k will be liter/cm^2-hr.

After integrating and simplifying this equation, we obtain

$$1-(1-F)^{1/3} = \left(\frac{3M\delta}{\phi r_g r_0 \rho_g}[SO_2]^p [O_2]^q k\right)t \tag{10}$$

or

$$1-(1-F)^{1/3} = (\text{Linear rate constant} / r_0)t \tag{11}$$

where

$$\text{Linear rate constant} = \frac{3M\delta[SO_2]^p[O_2]^q k}{\phi r_g \rho_g} \quad (12)$$

M = molecular weight of pyrite, (grams/mol)

r_g = average pyrite grain radius, (cm)

ρ_g = density of pyrite, (grams/cm^3)

F = fraction of iron minerals reacted

Effect of Temperature

The linear rate constant has a unit of cm/hr and is the velocity of the reaction zone movement. Figure 9 is a plot according to Equation (11); that is, a plot of $1-(1-F)^{1/3}$ vs. time at various temperatures. F represents the fraction of iron minerals reacted or the conversion that was calculated by the amount of iron in the solution divided by the total iron content of both pyritic and non-pyritic iron contained in the coal sample. As can be seen from Figure 9, the data points at various temperatures fit the linear relationship very well, confirming the validity of the chemical reaction-controlled model.

It is particularly interesting to note that the straight line at 73ºC in Figure 9 does not pass through the origin. This type of observation has been mentioned in the leaching study of zinc sulfide with a mixture of SO_2 and O_2.[5] This distinctive behavior at 73ºC is surmised to be a mechanism in which it takes a certain period of time to reach a steady state concentration of SO_2 that can leach coal pyrite according to the model.

The linear rate constants at various temperatures were obtained by multiplying the slopes of the straight lines in Figure 9 by r_0 value. These were plotted according to the Arrhenius equation and are shown in Figure 10. From the slope of the straight line, the activation energy was determined to be 11.6 kcal/mole. The magnitude of this activation

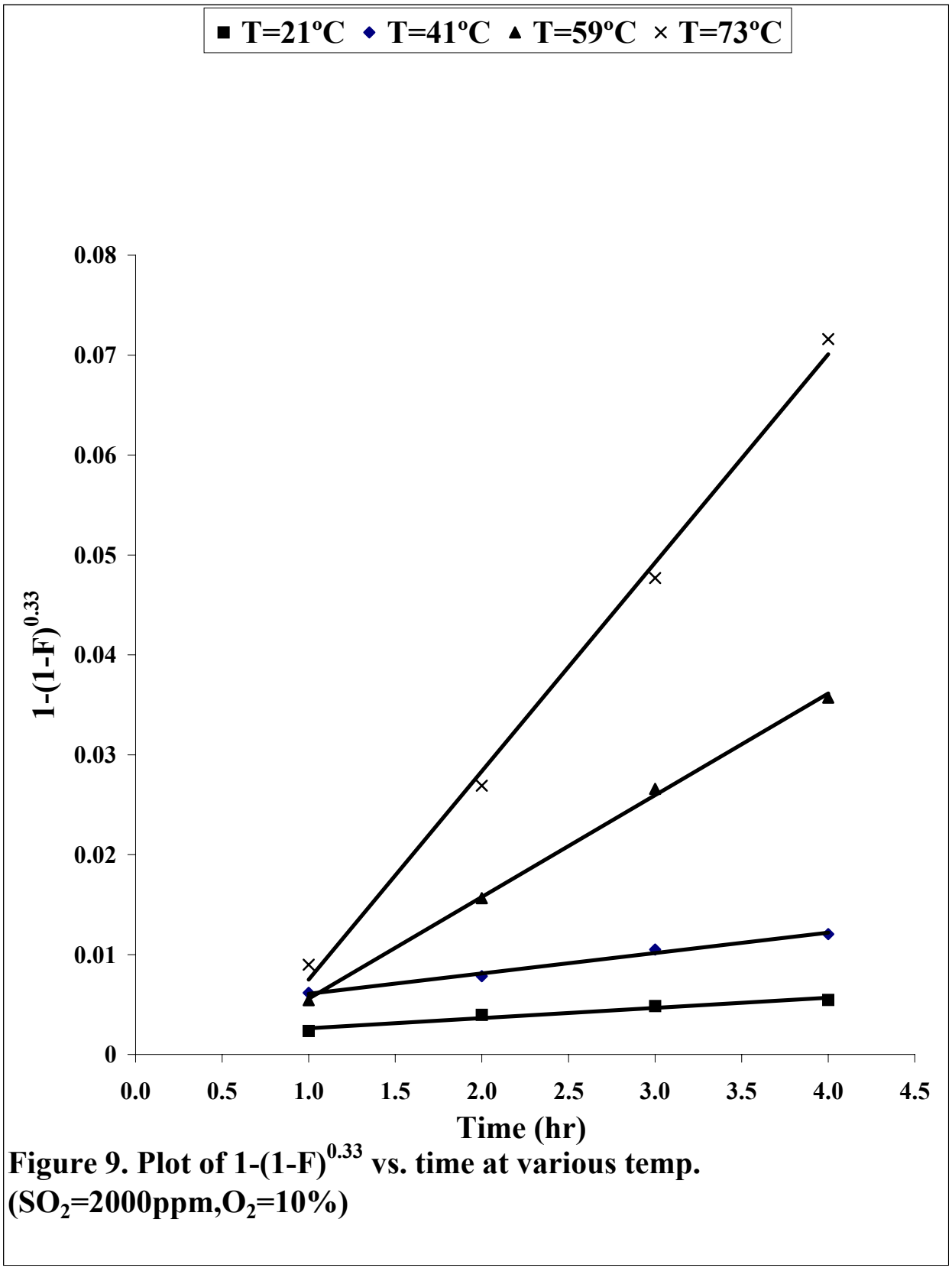

Figure 9. Plot of $1-(1-F)^{0.33}$ vs. time at various temp. (SO_2=2000ppm,O_2=10%)

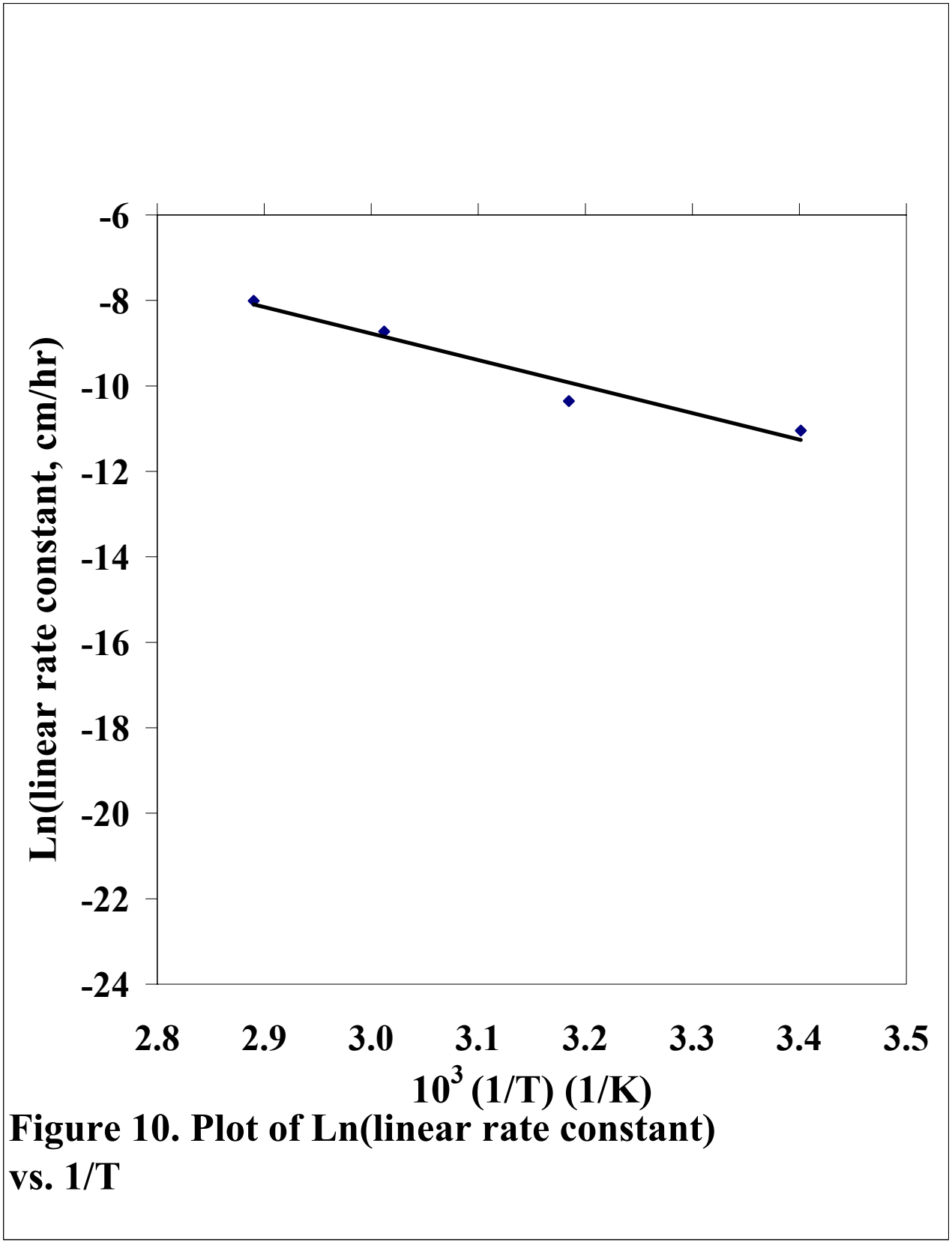

Figure 10. Plot of Ln(linear rate constant) vs. 1/T

energy confirms again the validity of the chemical reaction-controlled model used in this study. The activation energy, however, is not a real value but apparent activation energy because the concentration of aqueous SO_2 decreases as temperature increases. Thus, the real activation energy should be much higher than this value. This consideration is verified on the work conducted by Adams and Matthew.[5] They observed that the leaching rate of zinc sulfide with a mixture of SO_2 and O_2 increased with increasing temperatures up to about 85ºC then decreased with further increase in temperature. This phenomenon can be explained by the decrease in the solubility of SO_2 at elevated temperatures.

Effect of Oxygen Concentration

A plot of $1-(1-F)^{1/3}$ vs. time for various oxygen concentrations is shown in Figure 11. The linear rate constants obtained by multiplying the slopes of the straight lines in Figure 11 by r_0 value are plotted vs. oxygen concentration. The plot is shown in Figure 12. It can be seen that the linear rate constant increases as the oxygen concentration increases up to 10% and then tends to level off as the oxygen concentration further increases. It appears that the variation of linear rate constant with oxygen concentration is a reflection of a type of Langmuir adsorption equation. This trend with the oxygen effect has been observed previously in a leaching study of chalcopyrite in an ammoniacal solution with oxygen.[12]

They found that the leaching rate with respect to oxygen concentration on the mineral surface was half-order dependent. They also fitted the rate curves by an equation showing the half-order dependence of the surface oxygen concentration. The half-order reaction is characteristic of an electrochemical reaction and can be found elsewhere.[13]

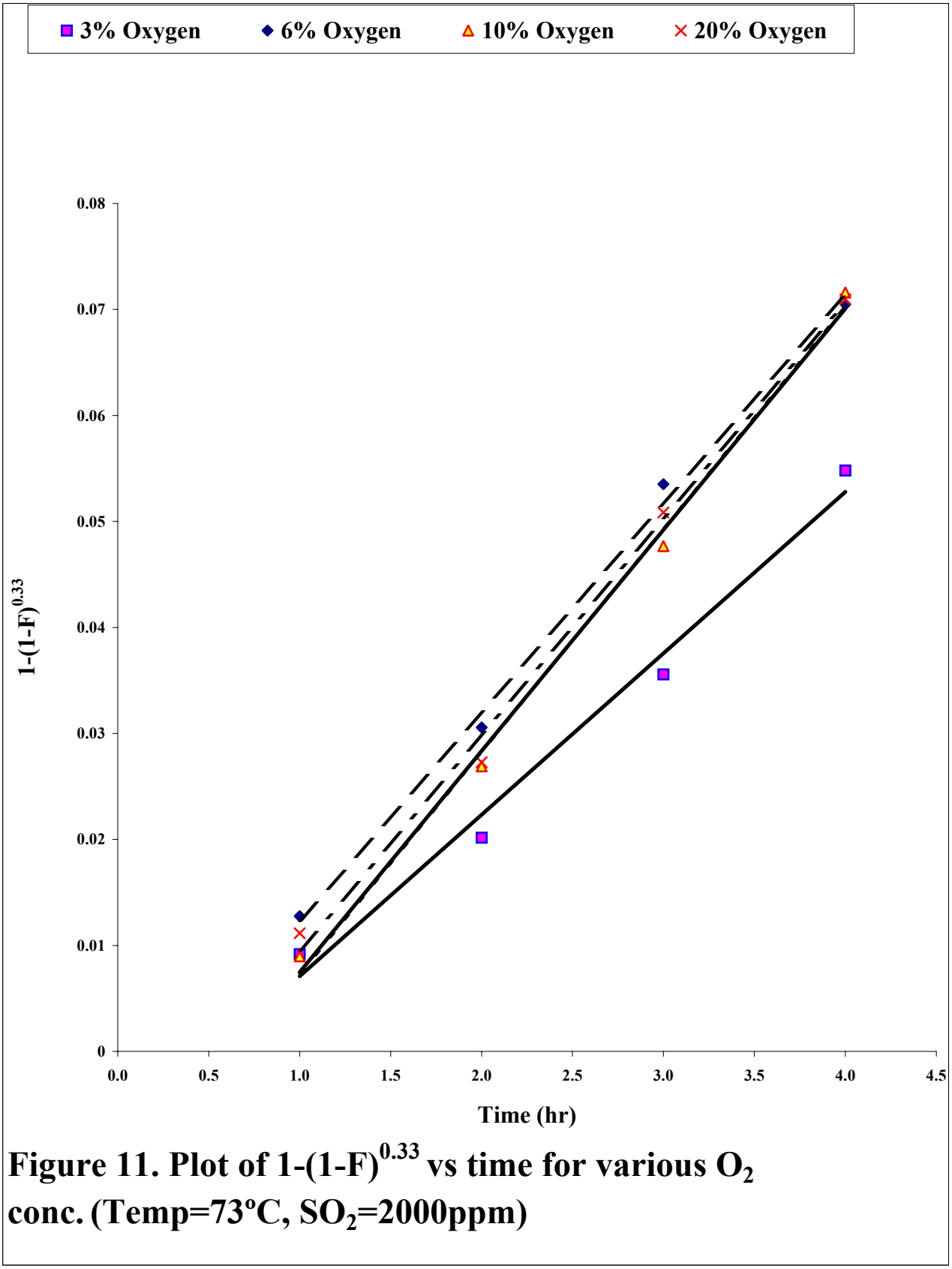

Figure 11. Plot of $1-(1-F)^{0.33}$ vs time for various O_2 conc. (Temp=73°C, SO_2=2000ppm)

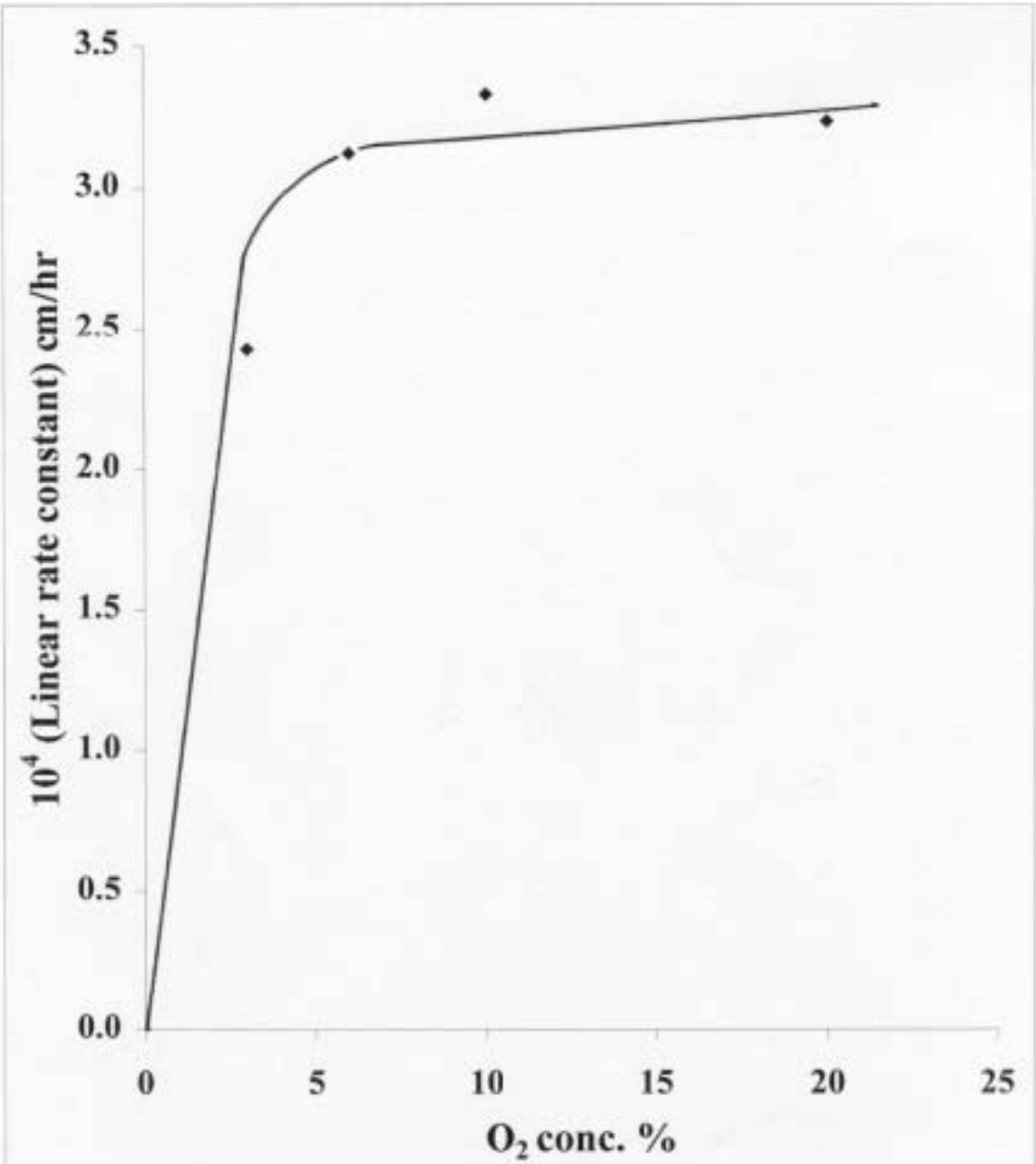

Figure 12. Effect of O_2 conc. on the linear rate constant (Temp=73°C, SO_2=2000 ppm)

The leaching reaction of coal pyrite with the combination of SO_2 and O_2 is undoubtedly an electrochemical reaction.

In the present study, an equation for linear rate constant in terms of oxygen concentration was determined by fitting the data. The equation was based on the Langmuir adsorption equation and half-order with respect to surface oxygen concentration. It takes the form

$$\text{linear rate constant} = C_1 \left(\frac{\frac{K_1 \times P}{100 H_1}[O_2]}{1 + \left(\frac{K_1 \times P}{100 H_1}[O_2] \right)} \right)^{1/2} \tag{13}$$

where

C_1 = constant

H_1 = Henry's constant for oxygen

P = total gas pressure

K_1 = equilibrium constant of the adsorption reaction of $[O_2]_{aq}$

$[O_2]$ = concentration of oxygen (%) in the gas stream

Note that the reaction order with respect to $[O_2]$ approaches half when $[O_2]$ is low and then it approaches zero when $[O_2]$ is high.

The quantity inside the parenthesis is related to surface oxygen concentration as shown

$$O_{2(s)} = O_{2(s)sat} \left(\frac{\frac{K_1 \times P}{100 H_1}[O_2]}{1 + \left(\frac{K_1 \times P}{100 H_1}[O_2] \right)} \right) \tag{14}$$

where

$O_{2(s)}$ = surface oxygen concentration

$O_{2(s)sat}$ = surface oxygen concentration at saturation

The fit as shown in Figure 12 was one of the better ones and resulted from the value of C_1 as 3.23×10^{-4} cm/hr and the value of $K_1\times P/100H_1$ as 0.8. It appears that Equation (13) can explain at least the trend with which the linear rate constant varies with O_2 concentration.

Effect of SO_2 concentration

A plot of $1-(1-F)^{1/3}$ vs. time for various SO_2 concentrations is shown in Figure 13. The linear rate constants were obtained the same way as before for oxygen concentrations. The linear rate constant is plotted against SO_2 concentration and the plot is shown in Figure 14. Again, the variation of linear rate constant with SO_2 concentration is a reflection of a type of Langmuir adsorption equation. This kind of trend with the SO_2 effect has been observed in the study of FeS dissolution in aqueous SO_2 solutions. [14]

The same analysis used for the effect of oxygen is used again to explain the variation of linear rate constant with SO_2 concentration. Then the rate equation would become

$$\text{linear rate constant} = C_2\left(\frac{\frac{K_2\times P}{100H_2}[SO_2]}{1+\left(\frac{K_2\times P}{100H_2}[SO_2]\right)}\right)^{1/2} \qquad (15)$$

where

C_2 = constant

K_2 = equilibrium constant of the adsorption reaction of $[SO_2]_{aq}$

H_2 = Henry's constant for SO_2

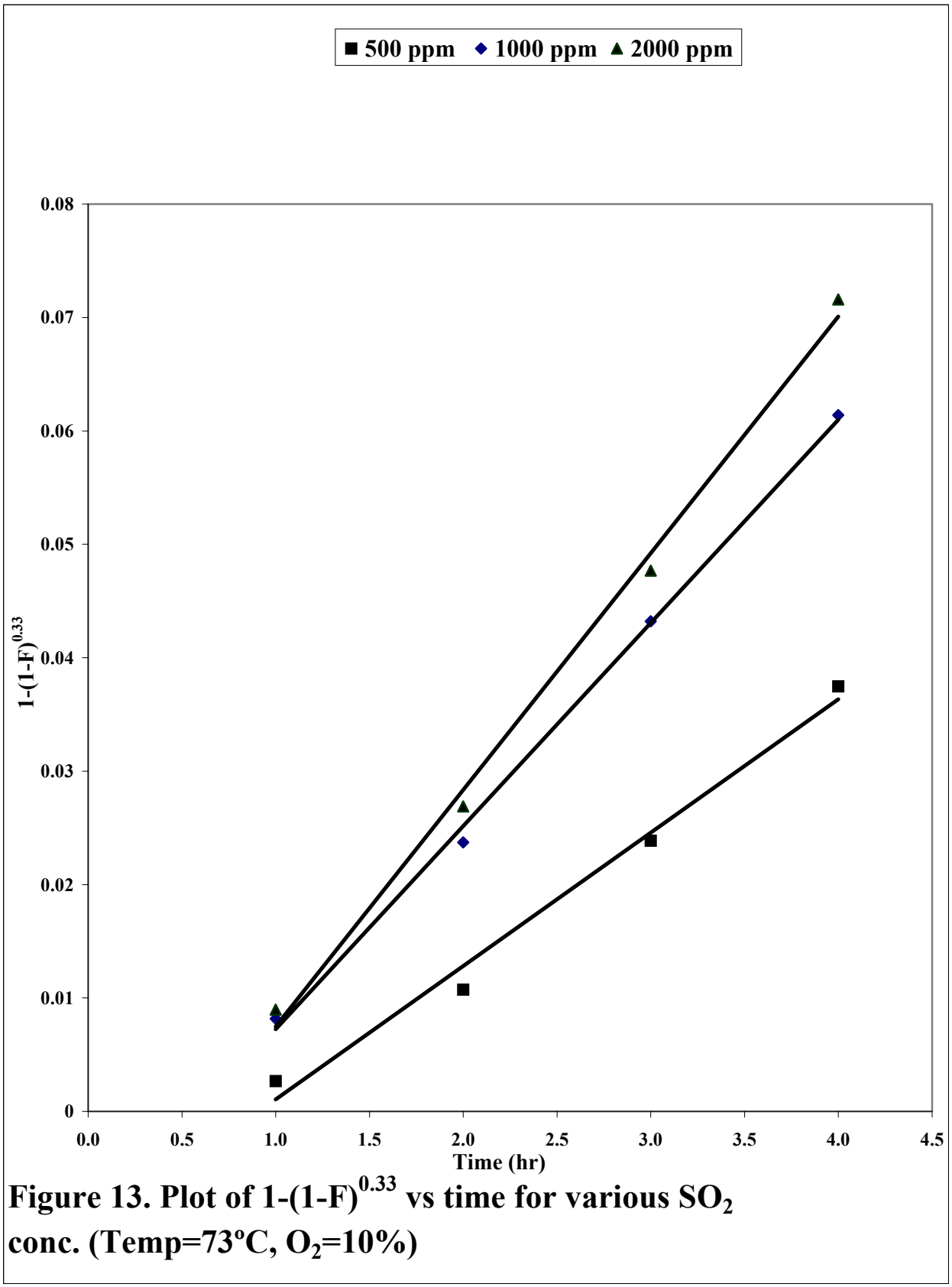

Figure 13. Plot of $1-(1-F)^{0.33}$ vs time for various SO_2 conc. (Temp=73°C, O_2=10%)

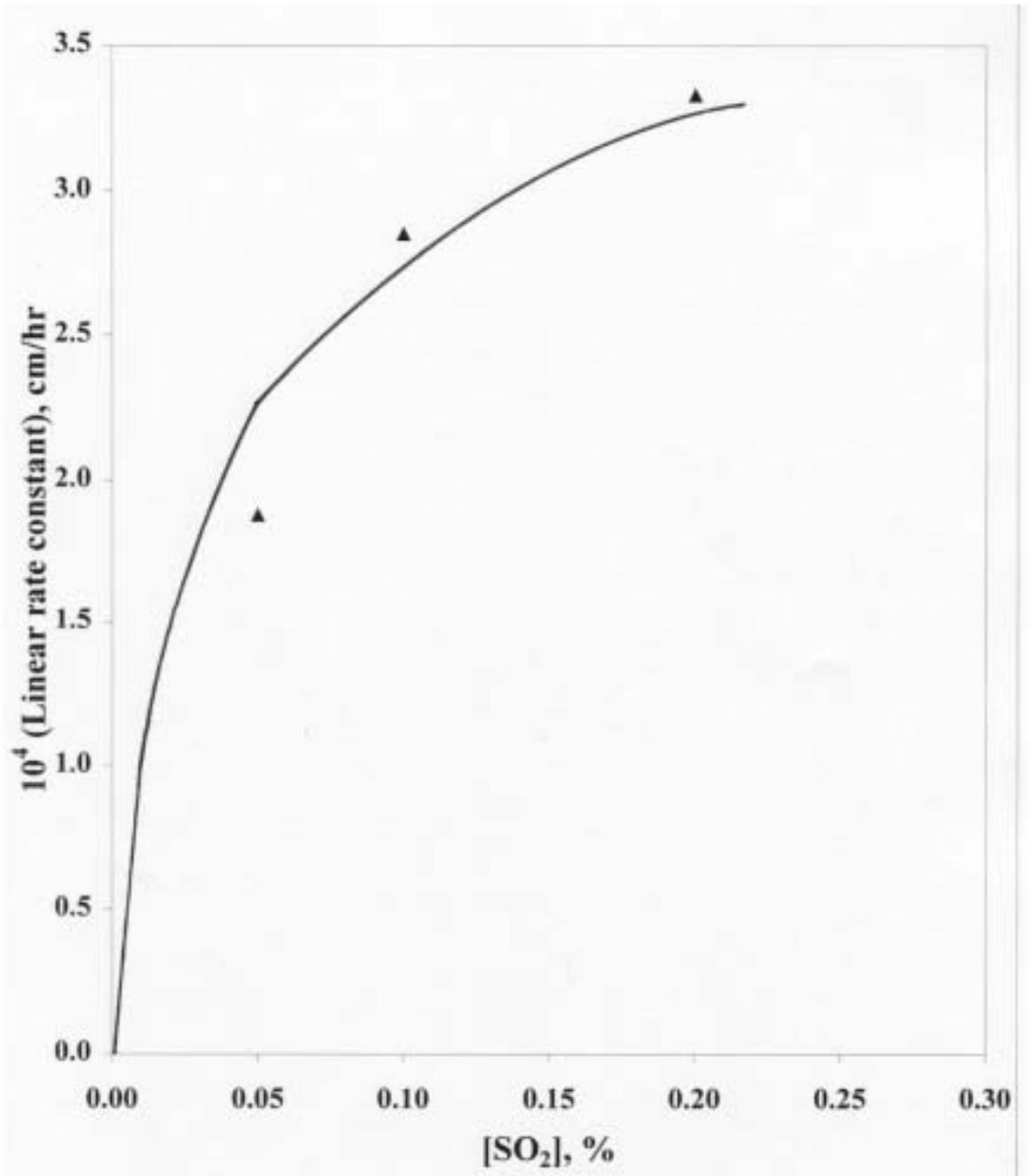

Figure 14. Effect of SO_2 conc. on the linear rate constant (Temp.=73°C, O_2=10%)

$[SO_2]$ = concentration of SO_2 (%) in the gas stream

Note that the reaction order with respect to $[SO_2]$ approaches half when $[SO_2]$ is low and then it approaches zero when $[SO_2]$ is high.

Equation (15) was used to fit the data and the result is shown in Figure 14. The fit was one of the better ones and resulted from the value of C_2 as 4×10^{-4} cm/hr and the value of $K_2\times P/100H_2$ as 9. It appears that Equation (15) can explain at least the trend with which the linear rate constant varies with SO_2 concentration.

CONCLUSIONS

From the experimental data the following conclusions were drawn:

1. Removal of SO_2 depends on the reaction temperature to a large extent. For example, the SO_2 recovery was 13.1% at 21^0C, 42.8% at 41^0C, 96.2% at 59^0C, 99.2% at 73^0C, all after 4 hours.
2. Removal of SO_2 is accomplished by the catalysis of iron, which was produced by leaching coal pyrite.
3. The coal pyrite is leached in the presence of oxidizing reagent, which is a combination of SO_2 and O_2.
4. Removal of SO_2 increases with increasing O_2 concentration up to 10% and levels of upon further increase.
5. The effect of SO_2 concentration on its removal is minimal.
6. The effect of O_2 concentration and SO_2 concentration on the leaching rate of coal pyrite follows a type of Langmuir adsorption equation.

REFERENCES

1. A. V. Slack, Sulfur Dioxide Removal from Waste Gases, 1971, Noyes Data Corporation, NJ, pp. 48-50.
2. Massaki Noguchi and Hideo Idemura, "Chiyoda SO_2 Removal Processes," in Sulfur Dioxide Control in Pyrometallurgy, edited by T. D. Chatwan and N. Kitumoto, The Metallurgy Society of AMIE, 1981, pp. 143-152.
3. Eung Ha Cho, "Removal of SO_2 with Oxygen in the Presence of Fe(III)," Met. Trans. B, vol. 17B, 1986, pp. 745-753.
4. Hun-Joon Sohn and Milton E. Wadsworth, "Reduction of Chalcopyrite with SO_2 in the Presence of Cupric Ions," Journals of Metals, Nov. 1980, pp. 18-22.
5. Robert W. Adams and Ian G. Mattew, "Leaching of Metal Sulfide Concentrates at Atmospheric Pressure Using SO_2 /O_2 Mixtures," Proc. Australas. Inst. Min. Metall. No.280, December 1981, pp. 41-52.
6. E. Peters and H. Majima, "Electrochemical Reactions of Pyrite in Acid Perchlorate Solutions," Canadian Metallurgy Quarterly, vol. 7, No. 3, 1968, pp. 111-117.
7. R.W. Lai, et al., "Comparitive Study of the Surface Properties and the Reactivity of Coal Pyrite and Mineral Pyrite," Preprint No. 89-6, also presented at the Annual AMIE Meeting at Las Vegas, Nevada, February 27-March 2, 1989.
8. Standard Methods of Chemical Analysis, Sixth edition, volume one, edited by N. H. Furman, D. Van Nostrand Company, Inc. New York (1966), pp. 1016-1017.
9. Annual Book of ASTM Standards, Gaseous Fuels; Coal and Coke, 1987, section 5, volume 05.05, pp. 336-340.

10. Annual Book of ASTM Standards, Gaseous Fuels; Coal and Coke, 1987, section 5, volume 05.05, pp. 385-388

11. Eung Ha Cho, Kevin H. Chang and Ronald R. Rollins, "A Kinetic Study of Leaching of Coal Pyrite with Nitric Acid," Metallurgical Transactions B, volume 14B, September 1983, pp. 317-324.

12. L. W. Beckstead and J. D. Miller, "Ammonia, Oxidation Leaching of Chalcopyrite-Reaction Kinetics" Metallurgical Transactions B, volume 8B, March 1977, pp. 19-29.

13. J. Brent Hiskey and Milton E. Wadsworth, "Galvanic Conversion of Chalcopyrite" Metallurgical Transactions B, volume 6B, March 1975, pp. 183-190.

14. G. B. Brual, J. J. Byerley and G. L. Rempel, " Kinetic and Mechanistic Study of FeS Dissolution in Aqueous Sulfur Dioxide Solution," Hydrometallurgy, vol. 9, 1983, pp. 307-331.

APPENDIX A

EXPERIMENTAL DATA

Figure 2. Overall removal of SO_2 for 4 hours at various temp.

(O_2=10%,SO_2=2000ppm)

Temperature (ºC)	Removal (%)
21	13.1
41	42.84
59	96.2
73	99.18

Figure 3. Plot of Fe conc. vs. time for various temperatures

(SO_2=2000ppm,O_2=10%)

Temperature (ºC)	Fe concentration (ppm)			
	Time (hr)			
	1	2	3	4
21	8.47	14.46	17.66	20.06
41	14.31	28.4	38.21	44.03
59	19.6	55.87	93.86	124.95
73	32.25	96.18	168.63	249.6

Figure 4. Overall removal of SO_2 for 4 hours at various O_2 conc.

(Temp.=73ºC,SO_2=2000ppm)

Oxygen Concentration (%)	Overall removal of SO_2 for 4 hours (%)
3	91.09
6	97.48
10	99.18
20	100

Figure 5. Overall removal of SO_2 for 4 hours at various SO_2 conc.

(Temp.=73ºC,O_2=10%)

SO_2 concentration (ppm)	Overall removal of SO_2 for 4 hours (%)
500	99.59
1000	98.29
2000	99.18

Figure 6. Linear dissolution rates of SO_2 at various temp.

(SO_2=2000ppm,O_2=10%)

Temp. (ºC)	Ln([SO_2(s)]/([SO_2(s)]-[SO_2]))						
	Time (min)						
	0	12	15	24	30	60	75
21	0	-	0.4161	-	0.8963	2.1604	2.6821
57	0	1.0413	-	2.8359	-	-	-
71	0	2.2998	-	-	-	-	-

Figure 7. Conc. of dissolved SO_2 Vs time at various rpm

(SO_2=2000ppm,O_2=10%,temp. =21ºC)

Rpm	[SO_2] (moles/liter)									
	Time (min)									
	12	15	24	30	36	45	48	60	75	90
504	0.0032	-	0.0037	-	0.006	-	0.0106	-	-	-
472	-	0.0043	-	0.0066	-	0.0081	-	0.0094	0.01	0.012
390	-	0.0041	-	0.0067	-	0.0080	-	0.0097	0.010	-

Figure 9. Plot of $1-(1-F)^{0.33}$ vs. time at various temp.

(SO_2=2000ppm,O_2=10%)

Temp. (ºC)	$1-(1-F)^{0.33}$			
	Time (hr)			
	1	2	3	4
21	0.0023	0.0040	0.0049	0.0055
41	0.0062	0.0078	0.0105	0.0120
59	0.0054	0.0157	0.0266	0.0357
73	0.0090	0.0269	0.0477	0.0716

Figure 10. Plot of Ln(linear rate constant) vs. 1/T

10^3 (1/T) (1/k)	Ln(linear rate constant, cm/hr)
3.4014	-11.0476
3.1847	-10.3545
3.0120	-8.7252
2.8902	-8.0079

Figure 11. Plot of $1-(1-F)^{0.33}$ vs time for various O_2 conc.

(Temp=73ºC, SO_2=2000ppm)

$[O_2]$ (%)	$1-(1-F)^{0.33}$			
	Time (hr)			
	1	2	3	4
3	0.0092	0.0202	0.0356	0.0548
6	0.0128	0.0306	0.0535	0.0705
10	0.0090	0.0269	0.0477	0.0716
20	0.0112	0.0273	0.0508	0.0710

Figure 12. Effect of O_2 conc. on the linear rate constant

(Temp=73ºC, SO_2=2000 ppm)

O_2 conc. (%)	10^4 (Linear rate constant) (cm/hr)
3	2.4206
6	3.1213
10	3.3283
20	3.2328

Figure 13. Plot of $1-(1-F)^{0.33}$ vs time for various SO_2 conc.

(Temp=7310^4, O_2=10%)

$[SO_2]$ (ppm)	$1-(1-F)^{0.33}$			
	Time (hr)			
	1	2	3	4
500	0.0027	0.0107	0.0239	0.0375
1000	0.0082	0.0237	0.0432	0.0614
2000	0.0090	0.0269	0.0477	0.0716

Figure 14. Effect of SO_2 conc. on the linear rate constant

(Temp.=73ºC, O_2=10%)

$[SO_2]$, %	10^4 (Linear rate constant), cm/hr
0.05	1.8792
0.1	2.8506
0.2	3.3283